Experimental comparison of rate-dependent hysteresis models in characterizing and compensating hysteresis of piezoelectric tube actuators

Omar Aljanaideh[a,*], Didace Habineza[b], Micky Rakotondrabe[b], Mohammad Al Janaideh[c]

[a]*Department of Mechanical Engineering, The University of Jordan, Amman 11942, Jordan*
[b]*The Department of Automatic Control and Micro-Mechatronic Systems, FEMTO-ST Institute, CNRS - University of Franche-Comt at Besanon, Besanon, France*
[c]*Department of Mechanical and Industrial Engineering, the Mechatronics and Microsystems Design Laboratory, The University of Toronto, Canada, and the Department of Mechatronics Engineering, The University of Jordan, Amman 11942, Jordan.*

Abstract

An experimental study has been carried out to characterize rate-dependent hysteresis of a piezoelectric tube actuator at different excitations frequency. The experimental measurements were followed by modeling and compensation of the hysteresis nonlinearities of the piezoelectric tube actuator using both the inverse rate-dependent Prandtl-Ishlinskii model (RDPI) and inverse rate-independent Prandtl-Ishlinskii model (RIPI) coupled with a controller. The comparison between both used methodologies is presented on through the modeling and compensation of the hysteresis of the actuator.

Keywords: Hysteresis, modeling, smart materials, piezo tube, dynamics, control.

1. Introduction

Piezoelectric tube actuators are considered attractive for micro-/nano- positioning and micro manipulating applications [1]. These actuators, however, similar to other types of smart actuators exhibit rate-dependent hysteresis nonlinearities that increase with the excitation frequency of the applied input [2–5]. Formulating a rate-dependent hysteresis model that can account the excitation frequency of the applied input is considered essential to expect the response of the actuator at various frequencies as well as to design controllers able to improve the tracking performance of smart actuators [6, 7]. Different methodologies have been proposed in the literature for characterizing the hysteresis nonlinearities. One of the the most popular methodologies is to employ a rate-independent hysteresis model (such as the classical Preisach, the classical Prandtl-Ishlinskii or the classical Bouc-Wen models [8, 9]) coupled with linear dynamics which is the so-called Hammerstein model. Another methodology suggested recently in the literature is to formulate a hysteresis model such as the Prandtl-Ishlinskii one in order to integrate the rate effect of the applied input in its parameters [10].

The primary goal of this study is to explore and compare the effectiveness of the rate-dependent Prandtl-Ishlinskii model (RDPI) and Hammerstein model in describing the dynamic hysteresis nonlinearities of piezoelectric actuator under different excitation frequencies. Since applying the inverse model would reveal the error due to characterization errors, a comparison is established on the basis of the compensation with an inverse RDPI [10] and with an inverse RIPI coupled with a controller [11]. A laboratory experiment was carried out to characterize the voltage-to-displacement characteristics under different excitation frequencies and experimental data were employed to identify the parameters of the used models.

2. Characterization of hysteresis nonlinearities of piezoelectric tube actuator

2.1. The experimental setup

The experimental setup is represented in Fig.1. It is composed of a piezoelectric tube able to deflect along two directions (X and Y directions), a computer with *Matlab/Simulink* software, two displacement sensors and two voltage amplifiers. In this experiment, only the Y axis deflexion is studied. The displacement sensors and voltage amplifiers are connected to the computer through a *dSPACE-1103* board. The piezoelectric tube scanner used is the PT230.94, fabricated by *Physik Instrumente* company. This tube has 30 *mm* of length, 3.2 *mm* of outer diameter and 2.2 *mm* of inner diameter. PT230.94 is made of PZT material coated by one inner electrode (in silver) and four external electrodes (in copper-nickel alloy), commonly named +x, -x, +y and -y (Fig.1)(a). Voltages U_y and $-U_y$ can be applied on +y and -y electrodes in order to bend the tube along Y-axis. To allow a linear displacement measurement (which is not possible with the tubular shape of the piezoelectric tube actuator), a small cube with perpendicular and flat sides is placed on the top of the tube. The operating voltage range of the PT230.94 is $\pm 250V$ for a deflection of $\pm 35\mu$m. Hence, voltage amplifiers are used to amplify the dSPACE board output voltages, for which the maximum range is about $\pm 10V$. The tube deflections are measured by using LC-2420 displacement sensors (from *Keyence* company), which are tuned to have 10nm resolution and a bandwidth of 50kHz. Note that these displacement sensors are used only for the characterization: the proposed control approach is exclusively feedforward and these

*Corresponding author
Email address: omaryanni@gmail.com (Omar Aljanaideh)

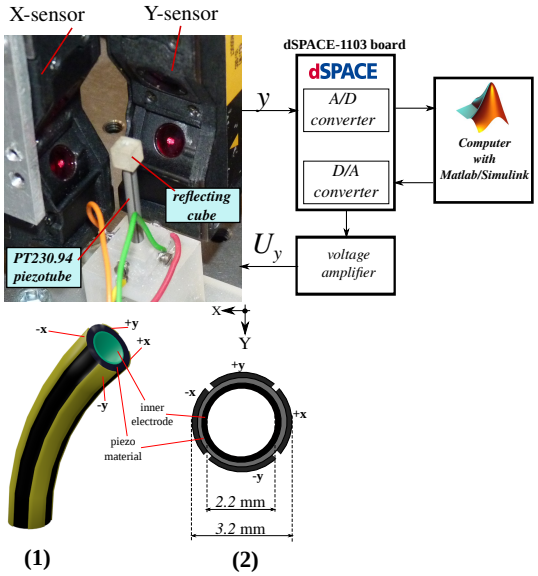

Figure 1: The figure shows the Experimental setup and description of the piezoelectric tube actuator, where (1) perspective view, and (2) top view.

sensors are not needed for tracking. Despite the capability of the actuator to move at least in two directions (XY scan), only the x-axis has been considered due to the scalar nature of the considered model.

The output displacement of the actuator was measured under sinusoidal input of $200V$ at 3 different excitations of frequency $f = 10, 50$, and 100 Hz. This range of frequency incorporates excitations where the hysteresis is relatively rate-independent (lower than 10 Hz) as well as rate-dependent (beyond 10 Hz). The output displacement of the piezoelectric actuator corresponding to each excitation frequency is illustrated in Fig.2(a). In addition, an experiment to measure the step response of the actuator was conducted to identify the dynamics of the actuator. Fig.2(b) displays the output displacement of the actuator under step input of $200V$. The identified dynamics of the actuator will be employed to synthesis a controller on the basis of an H_∞ controller. In the next section the measured data is used to identify the parameters of the used models.

3. Hysteresis modeling

The mathematical formulation of the RDPI and modeling based on the Hammerstein model is revisited in this section.

3.1. The rate-dependent Prandtl-Ishlinskii model

The model is presented in details in [10]. For a discrete-time input $u(k)$ and for $i = 1, 2, ..., n$, where $n \in \mathbb{N}$ and $j = 1, 2, ..., J$, the output of the RDPI model is given as the superposition of several weighted rate-dependent play operators as

$$\Gamma[u](j) := \rho_0 u(j) + \sum_{i=1}^{n} \rho_i \Phi[u](j), \qquad (1)$$

where ρ_i are constants representing the weights, Φ is the rate-dependent play operator with a dynamic threshold $r_i(v(j)) = \alpha_1 i + \alpha_2 |v(j)|$, where α_1 and α_2 are positive constants, and v is the rate of the applied input. o

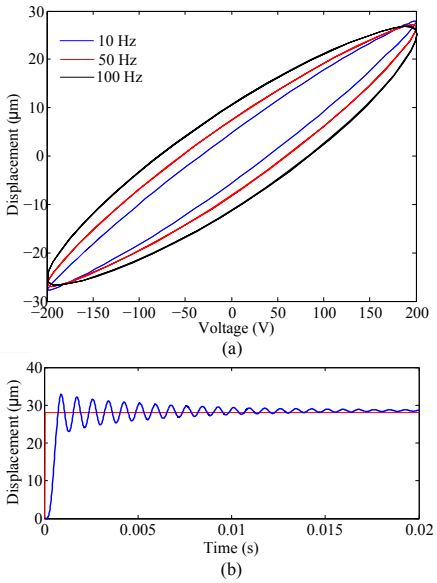

Figure 2: The output displacement of the actuator under harmonic input of 200 V at frequency 10, 50 and 100 Hz .

3.2. The Hammerstein model with the RIPI model

A rate-independent model coupled with a normalized linear dynamics (see Fig.3) is one of the popular methodologies to describe the rate-dependent hysteresis of smart actuators [13, 14]. Employing a cascade arrangement of the RIPI [8] and the identified dynamics can characterize the rate-dependent hysteresis of the actuator. The output of the RIPI is

$$\Delta[u](j) := \rho_0 u(j) + \sum_{i=1}^{n} \rho_i \Lambda[u](j), \qquad (2)$$

where Λ is the rate-independent play operator.

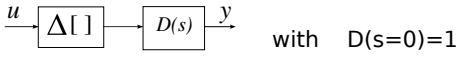

Figure 3: The Hammerstein model Π with the RIPI model Δ and the linear dynamics D.

3.3. Parameters identification

In order to investigate and compare the effectiveness of the RDPI model and the Hammerstein model Π in modeling the rate-dependent hysteresis of the piezoelectric tube actuator, the parameters of both models have to be identified on the basis of the laboratory-measured data. A minimization of the sum-squared error function was formulated to identify the parameter of the RDPI model, see [10] for more details. In order to examine the effectiveness of the model in describing the rate-dependent hysteresis nonlinearities, the model response is compared with the corresponding measured data in Fig.4.

By applying the ARMAX (Auto Regressive Moving Average with external inputs) parametric identification technique [15] to

the step response in Fig.2(b), a transfer function $G(s)$ is obtained. Normalizing this transfer function permits to get $D(s)$, i.e.: $D(s) = \frac{G(s)}{G(s=0)}$. Fig.5 displays a comparison between the dynamics of the actuator and the identified model $G(s)$ under the step input of $200V$ and Fig.6 shows the bode plot for $G(s)$. The parameters of the RIPI model were identified using the measured hysteresis loops under sinusoidal harmonic input of $200V$ at 0.1 Hz. The dynamics of the actuator $D(s)$ was coupled with the RIPI model Δ . The resulting output of the Hammerstein model Π is compared with the measured data from the piezoelectric tube actuator in Fig.7.

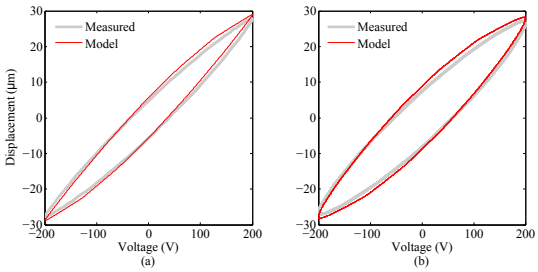

Figure 4: Comparison between the measured output displacement and Hammerstein model Π at: (a) 10, and (b) 50 Hz.

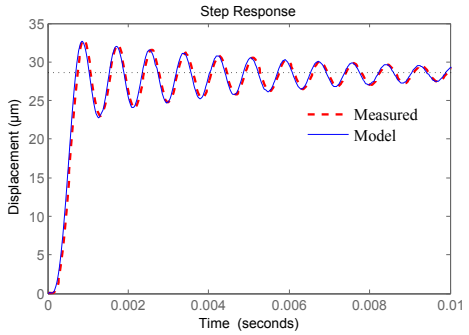

Figure 5: Comparison between the output of the piezoelectric tube actuator and the output of the identified model $G(s)$ when the step input $u(t) = 200V$ is applied.

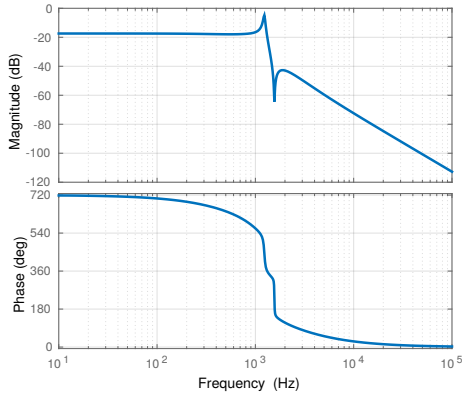

Figure 6: The bode plot for the linear dynamics $G(s)$.

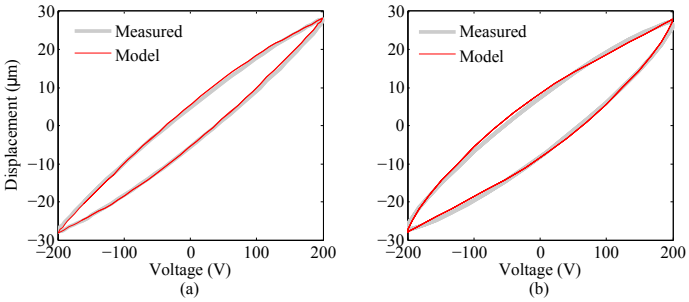

Figure 7: Comparison between the measured output displacement and RDPI Γ at: (a) 10 Hz, and (b) 50 Hz.

4. The compensators

4.1. Compensation with the inverse RDPI model

To compensate for the RDPI hysteersis model, an inverse RDPI model is employed. The output of the inverse is

$$u(k) = \Gamma^{-1}[y_r](k) = b_0 y_r(k) + \sum_{i=1}^{n} b_i \Phi[y_r](k), \tag{3}$$

where b_0 and b_i are constants and y_r the desired deflection. This inverse model is applied as feedforward compensator as shown in Fig.8 to compensate for the hysteresis nonlinearities [12].

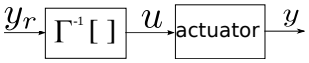

Figure 8: The inverse RDPI compensator.

4.2. Compensation with a H_∞ dynamic controller and an inverse RIPI model

If the dynamic hysteresis is modeled by the Hammerstein scheme, two compensators are proposed: first, an inverse RIPI Δ^{-1} that will compensates for the RIPI hysteresis, and then a compensator $K(s)$ for the linear dynamics $D(s)$ (see Fig.9a). Here, the approximate inverse RIPI in [8] is proposed for the hystersis and a H_∞ technique is proposed for K. The calculation of K necessitates to introduce weighting functions W_r, W_1 and W_2, see Fig.9b. In the H_∞ technique, these weighting functions are used to account for various specifications set for the compensated system. In our case, weightings W_r and W_1 are chosen based on the tracking performances (static error, bandwidth, etc) desired for the compensated system. The weighting W_2 is used to limit the control voltage, in order to avoid the saturation of the actuator (command moderation). The chosen weighting functions are

$$W_r(s) = \frac{1}{1 + \frac{0.01}{3}s}; \qquad W_1(s) = \frac{s + 120}{s + 1.2}; \qquad W_2(s) = 0.125. \tag{4}$$

From the augmented system in Fig.9b, the transfer between the exogenous input y_r and exogenous outputs z_1 and z_2, fictive signals used for the synthesis only, is expressed as

$$\begin{pmatrix} z_1 \\ z_2 \end{pmatrix} = \begin{pmatrix} W_2 K \\ W_1 W_r - W_1 T \end{pmatrix} d_r, \tag{5}$$

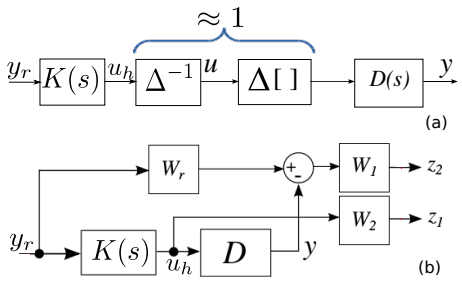

Figure 9: Compensation for the Hammerstein model. (a): the Hammertsein model compensated by the inverse RIPI hysteresis model and by a linear dynamic K. (b): H_∞ calculation of the dynamics controller K using weightings.

with $T = DK$ the transfer function of the compensated system. The standard H_∞ problem consists therefore in finding the controller K such that

$$\left\| \begin{matrix} W_2K \\ W_1W_r - W_1T \end{matrix} \right\|_\infty < \gamma \quad \text{or} \quad \begin{cases} \|K\|_\infty < \|W_2^{-1}\|_\infty \gamma \\ \|W_r - T\|_\infty < \|W_1^{-1}\|_\infty \gamma \end{cases}, \tag{6}$$

where γ represents the performances evaluation parameter. From this latter condition, we observe that W_2^{-1} is used to shape and bound the outputs of the compensator in order to avoid the actuator saturation, W_r to impose the behavior desired for the compensated system, and W_1^{-1} to bound the error between the desired behavior W_r and the overall compensated system $T = DK$. To solve the problem in 6, we have used the DGKF algorithm [16] and a feedforward compensator K (transfer function), with $\gamma = 0.929688$, was obtained.

5. Compensation of hysteresis nonlinearities

Fig.10(a) shows the compensation of the hysteresis nonlinearities of the piezoelectric tube actuator using the inverse RDPI model. In Fig.10(b), the result with the inverse RIPI model coupled with the H_∞ dynamics controller is presented. Since the RDPI model shows slightly better characterization, the inverse RDPI shows relatively better compensation results than those obtained using the inverse rate-independent model coupled with the controller.

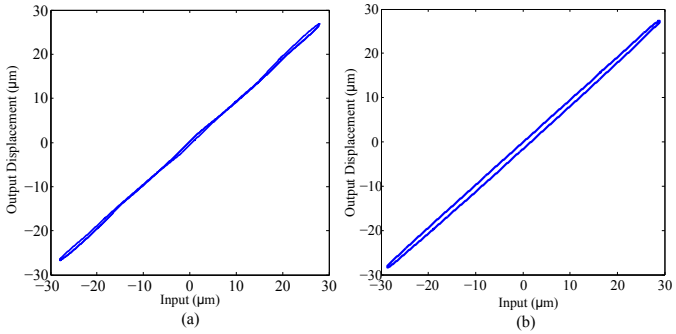

Figure 10: Compensation of hysteresis at excitation frequency of 10 Hz with (a) the inverse RDPI model, and (b) the H_∞ controller and the inverse RIPI model.

6. Conclusion

The measured output-input properties of a piezotube actuator show rate-dependent hysteresis nonlinearities that increase with the excitation frequency of the applied input voltage. These hysteresis nonlinearities were characterized using the RDPI model and with the Hammerstein model Π based on a linear dynamics and a RIPI model. The comparison revealed that both models show good agreement with the measured data at the operating range considered in the study. The inverse RDPI model and the H_∞ controller were also obtained for compensation of the rate-dependent hysteresis in order to evaluate the error due to characterization.

Acknowledgment

Work supported by the national ANR-JCJC C-MUMS-project (ANR-12-JS03007.01) and by the Labex-ACTION project (ANR-11-LABX-0001-01).

References

[1] D. Habineza, M. Rakotondrabe, and Y. Le Gorrec, "Bouc-Wen Modeling and Feedforward Control of Multivariable Hysteresis in Piezoelectric Systems: Application to a 3-DoF Piezotube Scanner," *IEEE Trans on Control System Technology*, vol.23(5), 2015, pp. 1797–1806.

[2] R. Smith, *Smart Material Systems: Model Development*, Society for Industrial and Applied Mathematics, 2005.

[3] M. Al Janaideh, C-Y. Su, and S. Rakheja, "Inverse generalized asymmetric Prandtl-Ishlinskii model for compensation of hysteresis nonlinearities in smart actuators," *IEEE Int Conf on Networking, Sensing and Control*, pp.834–839, Okayama, Japan, 2009.

[4] M. Al Janaideh, S. Rakheja, and C-Y. Su, A generalized Prandtl- Ishlinskii model for characterizing rate dependent hysteresis," *IEEE Int Conf on Control Applications*, pp.343–348, Singapore, Singapore, 2007.

[5] D. Davino, A. Giustiniani, and C. Visone, "The piezo-magnetic parameters of Terfenol-D: An experimental viewpoint," *Physica*, vol.407, pp.1427-1432, 2012.

[6] C. Visone, "Hysteresis modelling and compensation for smart sensors and actuators," *Journal of Physics: Conf Series*, vol.138, pp.1-25, 2008.

[7] O. Aljanaideh, M. Al Janaideh, S. Rakheja, and C-Y. Su "Compensation of Rate-Dependent Hysteresis Nonlinearities in a Magnetostrictive Actuator Using Inverse Prandtl-Ishlinskii Model," *Smart Materials and Structures*, vol. 22, no. 2, pp. 1-10, 2013.

[8] M. Rakotondrabe, 'Classical Prandtl-Ishlinskii modeling and inverse multiplicative structure to compensate hysteresis in piezoactuators', American Control Conference, pp.1646-1651, Montral Canada, June 2012.

[9] M. Rakotondrabe, 'Bouc-Wen modeling and inverse multiplicative structure to compensate hysteresis nonlinearity in piezoelectric actuators', IEEE Trans. on Automation Science and Engineering, Vol.8(2), pp.428-431, April 2011.

[10] M. Al Janaideh and P. Krejčí, "An inversion formula for a PrandtlIshlinskii operator with time dependent thresholds," *Physica B*, vol. 406, no. 8, pp. 1528-1532, 2011.

[11] M. Rakotondrabe, C. Clévy, and P. Lutz, "Complete open loop control of hysteretic, creeped, and oscillating piezoelectric cantilevers," *IEEE TRans on Automation Science and Engineering*, vol.7(3), pp. 440-450, 2010.

[12] O. Aljanaideh, M. Al Janaideh, and M. Rakotondrabe, "Enhancement of micro-positioning accuracy of a piezoelectric positioner by suppressing the rate-dependant hys- teresis nonlinearities," *IEEE/ASME Int Conf on Adv Intelligent Mechatronics*, pp.1683-1688, Besancon France, 2014.

[13] X. Tan, J. S. Baras, "Modeling and control of hysteresis in magnetostrictive actuators," *Automatica*, vol.40(9), pp. 1469-1480, 2004.

[14] D. Davino, C. Natale, S. Pirozzi, and C. Visone, "Phenomenological dynamic model of a magnetostrictive actuator," *Physica B*, vol. 343, pp. 112-116, 2004.

[15] L. Ljung, *System identification toolbox*, The Matlab user's guide, 1988.

[16] J. Doyle, K. Glover, P. Khargonekar, and B. Francis, "State-space solutions to standard H_2 and H control problems," *IEEE Trans on Automatic Control,* vol.34(8), pp.831-847, 1989.